# 7 Spatial Patterns in Biology

Spatial pattern is a fascinating aspect of biological systems, from the shape and size of organisms to the geographic distribution of species. Indeed, "morphogenesis," the generation of pattern, has long been regarded as one of *the* central problems of biology, and one that requires theory and models to address. The book *On Growth and Form* by D'Arcy Thompson, published in 1917, continues to be widely read and admired—a remarkable achievement in a discipline that has undergone rapid change. The conviction that morphogenesis is based upon mechanisms whose principles we can discover remains strong. The possible mechanisms can be classified in terms of the physical and/or chemical forces involved, or they can be classified in terms of the types of models that are used to reproduce observed patterns. Moreover, it is evident that different mechanisms operate in different systems. Rather than attempt to survey the different possibilities, we shall examine a single mechanism, called a reaction-diffusion system, and study two examples in which reaction-diffusion mechanisms have been shown to yield observed spatial patterns.

Reaction-diffusion models were proposed as an explanation of morphogenesis by Alan Turing in his last paper. Turing was a remarkable individual who was at the center of British efforts to break German codes during World War II. This work has been dramatized in novels, film, and plays (Hodges 2000). Turing also invented the *Turing machine*, now one of the fundamental concepts in computer science. In the work that we discuss here, Turing hypothesized that the combination of molecular diffusion and chemical reaction of substances he called *morphogens* could lead to instabilities in the homogeneous distribution of these substances (Turing 1952). While Turing describes three biological examples of morphogenesis (the tentacles of hydra, gastrulation, and the whorl patterns of plants such as woodruff), his work did not include analysis of data from these systems.

Many attempts have been made subsequently to demonstrate that Turing mechanisms are responsible for the creation of patterns in different systems.

Some of these have been successful, but there are natural patterns in which other forces also play a critical role in the pattern formation. To cite one example, Odell and Oster (1980) investigated the role of traction and mechanical forces in the process of gastrulation. Even in the cases in which reaction and diffusion do provide the primary basis for pattern formation, identification of the morphogens and their reactions with each other has required years of effort by many investigators. Nonetheless, certain patterns displayed by reaction-diffusion systems are very robust. These patterns can be studied in relatively simple reaction systems and the insight gained from them can be used to guide experimental research that seeks to elucidate the details of the biological mechanisms of different pattern-forming systems.

## 7.1 Reaction-Diffusion Models

Diffusion is the process by which the random motion of molecules due to thermal fluctuations leads to changes in the concentration of chemical species in space and time. We will talk later about animal species, and why diffusion models are often good approximations to their movements. There are two approaches to the derivation of the equations that describe diffusion. The first (historically) starts at the "macroscopic" level, treating chemical concentrations as smoothly varying functions of space and time, and making assumptions about the net behavior of large numbers of molecules in solution. A more fundamental and general approach is based on a "microscopic"-level analysis of individual molecules.

To introduce the individual approach, we begin with a *lattice model*. Consider the integer-valued points on the real line, and a molecule jumping randomly among these points. During each time step from $t$ to $t+1$, the molecule randomly takes a step to one of the two neighboring points, moving right or left with equal probability. This model is an example of a one-dimensional *random walk*. It is a caricature of the fact that in liquids and gases, molecules are constantly in motion, changing direction as they collide with one another. This *Brownian motion* was discovered in the nineteenth century by Robert Brown who observed the motion of pollen grains floating in water with a microscope.

The outcome of this random-walk diffusion model is summarized by the probability distribution of the particle's location. Let $X_n$ denote the particle's location after $n$ time units, starting from $X_0 = 0$. The choice of random steps to the right and left can be generated by tossing a fair coin $n$ times, assigning a right step to $H$ and a left step to $T$. Let $R$ and $L$ be the total number of steps to the right and left. If at the end of $n$ steps the particle is at location $k$, we then have

$$\begin{aligned} R + L &= n \\ R - L &= k \end{aligned} \qquad [7.1]$$

and hence $2R = n + k \Rightarrow R = (n + k)/2$ [note that $n$ and $k$ must either be both even, or both odd, since $R$ is an integer: after an even (odd) number of steps the particle is at an even (odd) location]. The probability that $X_n = k$ is therefore given by the binomial formula for the probability of getting $(n + k)/2$ $H$'s in $n$ tosses of a fair coin,

$$Pr\{X_n = k\} = \begin{pmatrix} n \\ (n+k)/2 \end{pmatrix} \left(\frac{1}{2}\right)^n. \qquad [7.2]$$

This holds for $|k| \leq n$ with $k$ and $n$ either both even or both odd, otherwise $Pr\{X_n = k\} = 0$.

We study approximations of [7.2] for large $k$ and $n$ via the central limit theorem. The central limit theorem is a generalization of the DeMoivre-LaPlace limit theorem for the binomial distribution that applies to more general models than the simple random walk. For our randomly walking particle, let $z_j$ be the change in location on the $j$th step, so that

$$X_n = z_1 + z_2 + \cdots + z_n.$$

Each of the $z$'s is independent of the others, and they all have the same probability distribution of possible values, $\pm 1$ with equal probability $1/2$. Consequently they all have the same mean $E[z] = 0$, and variance $\mathrm{Var}(z) = E[z^2] - E[z]^2 = 1 - 0 = 1$. The central limit theorem states that for a sum $X_n$ of $n$ independent and identically distributed random variables with common mean $\mu$ and variance $\sigma^2$, the distribution of $(X_n - n\mu)/\sqrt{n}\sigma$ converges to a Gaussian (normal) distribution with mean 0 and variance 1. Informally, we express this by saying that the distribution of $X_n$ is approximately Gaussian with mean $n\mu$ and variance $n\sigma^2$.

For our random walk model, we therefore conclude that the particle's location after $n$ steps has an approximately Gaussian distribution, with mean and variance

$$E[X_n] = 0, \qquad \mathrm{Var}[X_n] = n. \qquad [7.3a]$$

The central limit theorem also applies to more general situations where exact binomial calculations are no longer easy. For example, suppose that at each time-step jumps to the left or right of some fixed size $w > 0$ each occur with probability $p \leq 1/2$, and the particle stays put with probability $1 - 2p$. In this case $z_j$ has three possible values $(-w, 0, w)$. We still have $E[z_j] = 0$, but now $\mathrm{Var}(z_j) = 2pw^2$; hence $X_n$ is approximately Gaussian distributed with mean and variance

$$E[X_n] = 0, \qquad \mathrm{Var}[X_n] = 2pw^2 n. \qquad [7.3b]$$

**Exercise 7.1.** Suppose that at each time-step the particle can move to the right with probability $p$ and to the left with probability $q$ where $p + q \leq 1$. Assuming steps are of fixed size $w$, generalize [7.3b] (which applies if $p = q$) to this situation (and note that if $p \neq q$ the walk is biased: $E[z_j] \neq 0$).

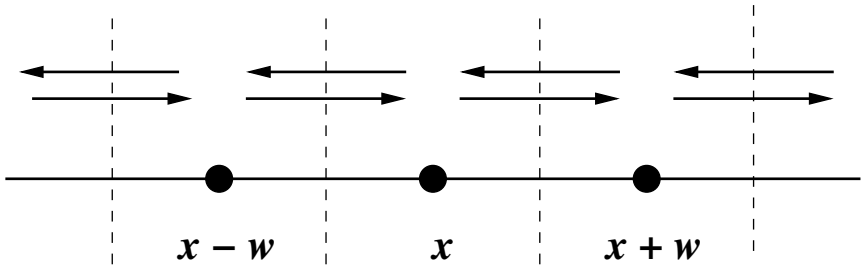


**Figure 7.1** Depiction of particles undergoing a random walk on the line with general step-size $w$.

The random walk model has the advantage of simplicity, but space is not a lattice, so we want continuous analogs for this analysis of random walks. To get a continuous model we will scale down the increments of time and distance to 0 in such a way that the distribution of particle locations approaches a limit. Specifically, we suppose that a move of length $w$ to the left or right can occur every $h$ units of time, with $p \leq 1/2$ being the probability of a move in each direction, see Figure 7.1. The Gaussian approximation [7.3b] tell us how $w$ and $h$ should be related to each other, in order to reach a limit: the variance in a particle's location at time $t$ has to remain the same. The number of steps up to time $t$ is $n = t/h$ so the variance is

$$2pw^2n = 2pw^2/h \times t = 2Dt \qquad [7.4]$$

where we have defined $D = pw^2/h$. Thus, we rescale so that $D$ remains constant (or at least approaches a limiting value as $w, h \to 0$).

We also consider the overall behavior of a large number of particles, obeying the same random walk model but moving independently of each other. Let $C(x,t)w$ be the number of particles in the interval centered on $x$ (between the dashed vertical lines surrounding $x$ in Figure 7.1); thus $C(x,t)$ is the "concentration at $x$" at time $t$, the number of particles per unit area. As a result of the moves that occur between $t$ and $t+h$ we then have

$$C(x,t+h)w = C(x,t)w - 2pC(x,t)w + p[C(x-w,t)w + C(x+w,t)w]. \qquad [7.5]$$

That is, the number in the interval at time $t+h$ is the number there at time $t$, minus those who leave, plus those who move in. The expressions in [7.5] for the numbers of moving particles are really the expected number (total number of particles $\times$ the probability of a move); by ignoring deviations from the expected number we are tacitly assuming that there are "many" particles in each compartment, even when $C$ is small.

Now we do Taylor series expansions of $C$ in space and time,

$$\text{(a)} \quad C(x,t+h) - C(x,t) = \frac{\partial C}{\partial t}(x,t)h + O(h^2)$$

$$\text{(b)} \quad C(x+w,t) - C(x,t) = \frac{\partial C}{\partial x}(x,t)w + \frac{\partial^2 C}{\partial x^2}(x,t)\frac{w^2}{2} + O(w^3) \qquad [7.6]$$

$$\text{(c)} \quad C(x-w,t) - C(x,t) = \frac{\partial C}{\partial x}(x,t)(-w) + \frac{\partial^2 C}{\partial x^2}(x,t)\frac{(-w)^2}{2} + O(w^3).$$

Equation [7.5] says that $(a) = p \times [(b) + (c)]$. Expressing this in terms of the right-hand sides of [7.6], we get that

$$\frac{\partial C}{\partial t}(x,t)h + O(h^2) = pw^2\frac{\partial^2 C}{\partial x^2}(x,t) + O(w^3).$$

Rearranging, and recalling that $pw^2/h = D$, we get

$$\frac{\partial C}{\partial t}(x,t) + O(h) = D\frac{\partial^2 C}{\partial x^2}(x,t) + O(w^3/h).$$

Finally we let $h, w \to 0$ with $D = pw^2/h$ constant. Since $w^3/h = Dw/p$, the $O(w^3/h)$ term goes to 0, and we get the *diffusion equation*

$$\frac{\partial C}{\partial t}(x,t) = D\frac{\partial^2 C}{\partial x^2}(x,t). \qquad [7.7]$$

This equation is a continuous description of the law of diffusion for particles undergoing Brownian motion on the line. To relate this back to the random walk model, consider the situation where there is a single particle (so the integral of $C$ over space is equal to 1 at all times), starting at location 0. A direct calculation shows that

$$p(x,t) = \left(\frac{1}{4\pi Dt}\right)^{1/2} \exp\left(\frac{-x^2}{4Dt}\right) \qquad [7.8]$$

is a solution to [7.7] with these properties. This is the formula for a Gaussian distribution with mean zero and variance $2Dt$, which is exactly the Gaussian approximation for the underlying random walk model.

In the plane, the corresponding equation for the concentrations $C(x,y,t)$ of Brownian motion particles is

$$\frac{\partial C}{\partial t} = D\left(\frac{\partial^2 C}{\partial x^2} + \frac{\partial^2 C}{\partial y^2}\right). \qquad [7.9]$$

The simple form of this equation results from the fact that motion in the vertical direction is independent of the motion in the horizontal direction. Similar to our one-dimensional equation, this can be derived by dividing the plane up into squares of side $w$, writing the balance equation for the numbers of particles moving into and out of each box, and scaling space and time in a way that preserves a Gaussian approximation for the distribution of individual particles.

To reach these simple equations we have made the heroic assumptions that particles take steps of fixed size, at fixed time intervals. Nonetheless, there is considerable experimental evidence supporting these equations as a quantitatively accurate description of Brownian diffusion. One reason for this is that our assumptions can actually be relaxed considerably—for example, by allowing particles to have a probability distribution of step lengths, that might correspond to the free path of a Brownian particle between one collision and the next, or the flight distance of an insect moving from one flower to another in a field. In that case, the simple diffusion equation emerges as the leading-order terms in an expansion involving higher-order derivatives in space (e.g., Goel and Richter-Dyn 1974), so long as conditions are homogeneous in space. A second reason is the central limit theorem, which yields a Gaussian approximation depending only on the mean and variance of the displacements in each unit of time, and how displacements in successive time intervals are correlated with each other. Over a macroscopic time span long enough that many steps occur, any "microscopic" model that gets these ingredients right, necessarily leads to the same approximate Gaussian distribution for the long-term distribution, and hence to the same partial differential equation for the concentration profile of many such particles. Thus, the long-term spread of some animal populations is described well by a simple two-dimensional diffusion model, even though the underlying assumptions about individual movement steps are rarely satisfied (Turchin 1998). However, the diffusion model fails when animals exhibit distinct short-range and long-range movement behaviors, so that the macroscopic displacements on the time scale of interest may result in part from a small number of large moves, leading to non-Gaussian patterns of spread. A third, related reason is that the diffusion equation can be derived from macroscopic-level properties. In particular the same balance equation [7.5] results from *Fick's Law of Diffusion*, which asserts that the rate of material flux across a surface (e.g., the dashed vertical lines in Figure 7.1) is proportional to the concentration gradient across the surface (see, e.g., Berg 1983 or Edelstein-Keshet 1988 for a derivation of the diffusion equation from Fick's Law). So any microscopic model which implies Fick's Law will again yield the same diffusion equation.

*Boundary conditions* are an important ingredient in obtaining a well-posed initial value problem for the diffusion equation. If our particles are random-walking within a bounded interval $I$ on the line, or a bounded spatial area $A$ in the plane, the diffusion equation does not specify what happens when particles reach the boundary. Additional boundary conditions must be imposed for there to be a unique solution to the diffusion equation. The appropriate boundary conditions reflect properties of the biological system being modeled. Two common boundary conditions are *no flux*, and *constant concentration* (in time). No-flux boundary conditions correspond to a situation where particles cannot move across the boundary. The equations describing this are that the directional derivative of the

concentration, in the direction perpendicular to the boundary, is identically 0. In the case of an interval $I = [a, b]$ on the line, no-flux boundary conditions are simply

$$\frac{\partial C}{\partial x}(x, t) \equiv 0 \text{ at } x = a \text{ and } x = b.$$

Constant boundary conditions arise when the concentration at the boundary is fixed by external conditions. For example, the region of interest may be immersed in a large reservoir of fluid which is well mixed and maintains a constant concentration. Particles can move across the boundary, but the external reservoir is so large that there is no significant change in its concentration of particles due to this movement. For example, the ion fluxes of membrane currents can be small enough that they make little change in intracellular or extracellular concentrations of the ions.

In the absence of spatial variation in concentrations, systems of equations for chemical reactions have the form

$$\dot{c}_i = f_i(c_1, \ldots, c_k).$$

Here $c_i$ is the concentration of species $i$, there are $k$ species altogether and the $f_i$ give the rate of change of $c_i$ due to chemical reactions. A reaction-diffusion model assumes that chemical concentrations may vary in space, and that the changes in chemical concentrations at a given location come from both chemical reactions and diffusion. In two space dimensions the model is

$$\frac{\partial c_i}{\partial t} = f_i(c_1, \ldots, c_k) + D_i \left( \frac{\partial^2 c_i}{\partial x^2} + \frac{\partial^2 c}{\partial y^2} \right) \qquad [7.10]$$

where each $c_i$ is a function of $(x, y, t)$.

## 7.2 The Turing Mechanism

Diffusion is a force that acts to homogenize concentrations. An initial distribution of concentrations will evolve to a spatially uniform state if diffusion is the only force acting on a substance and the boundary conditions are compatible with constant concentration in the interior of a domain. Therefore, it is surprising that instability of a reaction-diffusion system can give rise to spatial pattern for initial concentrations that are close to a stable equilibrium of the reaction system alone. Intuition says that diffusion should make things spatially smoother and more stable. The discovery that diffusion can destabilize an otherwise stable equilibrium was made by Alan Turing in 1952. We give one version of his argument here.

The systems we will consider are reaction-diffusion equations for a pair of chemical species on the unit circle. The circle is used as a domain because it is one dimensional, compact, and has no boundary. We further assume that the kinetic equations for the chemical reactions have a stable steady state and have been linearized about that state. Letting $u_1(x,t)$ and $u_2(x,t)$ represent the *departures* of the chemical concentrations from their steady-state values, we obtain equations of the form

$$\begin{aligned} \frac{\partial u_1}{\partial t} &= a_{11}u_1 + a_{12}u_2 + D_1\left(\frac{\partial^2 u_1}{\partial x^2}\right) \\ \frac{\partial u_2}{\partial t} &= a_{21}u_1 + a_{22}u_2 + D_2\left(\frac{\partial^2 u_2}{\partial x^2}\right) \end{aligned} \qquad [7.11]$$

for the linearized system. Here $x$ is the angular coordinate along the circle and the $u_i$ satisfy periodic boundary conditions $u_i(x+2\pi,t) = u_i(x,t)$ since $u_i$ is a function on the circle.

Now $u_1(x,t) = u_2(x,t) \equiv 0$ is a solution of this system that represents the homogeneous steady-state concentrations. We want to investigate the stability of this steady state, looking for instabilities of the homogeneous steady state that give rise to spatial patterns. This is more difficult than studying the stability of equilibria for ordinary differential equations because the state of the system at each time is a pair of functions $(u_1(x), u_2(x))$ describing the spatial distribution of concentrations. We can think of the set of possible concentration functions $(u_1(x), u_2(x))$ as forming an infinite dimensional phase space space and the partial differential equations [7.11] as defining a vector field on this phase space. Theorems about existence and uniqueness of solutions are more complicated in this infinite-dimensional context, but we plunge ahead anyway.

The equations are linear, so we seek solutions constructed from the eigenvalues and eigenvectors of the right-hand side of the equations. Since the states of the system are functions, the eigenvectors of this problem are called eigenfunctions. To find eigenfunctions, we utilize the fact that

$$\frac{d^2\sin(nx)}{dx^2} = -n^2\sin(nx).$$

Of course, a similar formula holds for $\cos(nx)$. Substituting

$$(w_1(t)\sin(nx), w_2(t)\sin(nx)) = (u_1(x,t), u_2(x,t))$$

into the reaction diffusion equation gives

$$\frac{dw_i}{dt}\sin(nx) = (a_{i1}w_1 + a_{i2}w_2 - n^2 D_i w_i(t))\sin(nx)$$

for $i = 1, 2$. We conclude that the functions whose spatial dependence is $\sin(nx)$ comprise a two-dimensional space that is *invariant*: solutions with initial conditions in this space stay in the space. Dividing the last equations by $\sin(nx)$ removes the $x$ dependence and leaves us with the pair of linear differential equa-

tions

$$\frac{dw_1}{dt} = a_{11}w_1 + a_{12}w_2 - n^2D_1w_1$$
$$\frac{dw_2}{dt} = a_{21}w_1 + a_{22}w_2 - n^2D_2w_2 \qquad [7.12]$$

for the coefficients $w_1(t), w_2(t)$ of spatial patterns whose spatial dependence is $\sin(nx)$. If the origin is a stable equilibrium of this system, then initial conditions will decay to the zero solution. On the other hand, if the origin is an unstable equilibrium then nonzero initial conditions of the form $(w_1(0)\sin(nx), w_2(0)\sin(nx))$ yield solutions of [7.11] that grow in amplitude.

The matrix of equation [7.12] is

$$A(n) = \begin{pmatrix} a_{11} - n^2D_1 & a_{12} \\ a_{21} & a_{22} - n^2D_2 \end{pmatrix}. \qquad [7.13]$$

Note that $n = 0$ gives the matrix for homogeneous perturbations to the zero solution of [7.11] and corresponds to the stability of the steady state for the reaction equations with no diffusion.

Spatial patterns will arise if the spatially homogeneous steady state is stable against spatially homogeneous perturbations ($n = 0$), but is unstable against some spatially inhomogeneous perturbations ($n > 0$). Our goal, therefore, is to analyze [7.13] to determine when this situation can occur.

There will be stability against homogeneous perturbations if all eigenvalues of $A(0)$ have negative real part. That is, we must have

$$a_{11}a_{22} - a_{12}a_{21} > 0 \text{ (positive determinant) and } a_{11} + a_{22} < 0 \text{ (negative trace).}$$

We next seek a value of $n$ with $A(n)$ having an eigenvalue with positive real part. The trace of $A(n)$ is $a_{11} + a_{22} - n^2(D_1 + D_2)$ which decreases with $n$. So the trace of $A(n)$ is negative for all $n$. Thus the only way to create a matrix with positive eigenvalue is to have the determinant become negative:

$$a_{11}a_{22} - a_{12}a_{21} - n^2(D_1a_{22} + D_2a_{11}) + n^4D_1D_2 < 0.$$

If $D_1 = D_2$, this too is impossible because $a_{11} + a_{22} < 0$ and the determinant increases with $n$. However, Turing observed that with diffusion constants $D_1$ and $D_2$ that differ, the determinant may become negative for positive values of $n$. For example, if we set $a_{11} = 1$, $a_{12} = -6$, $a_{21} = 1$, $a_{22} = -4$, $D_1 = 0.5$, $D_2 = 10$, and $n = 1$, then

$$A(1) = \begin{pmatrix} 0.5 & -6 \\ 1 & -14 \end{pmatrix},$$

which has determinant $-1$ but $a_{11}a_{22} - a_{12}a_{21} = 2 > 0$ and $a_{11} + a_{22} = -3 < 0$. It is easily seen that the signs of the reaction coefficients $a_{11}$ and $a_{22}$ must be opposite in any example of the Turing mechanism. This example demonstrates

that diffusion can destabilize a homogeneous stable steady state for a system of chemical reactions.

These observations on the conditions required for the Turing mechanism are the starting point for a class of reaction-diffusion models based upon local activation and long-range inhibition, introduced by Gierer and Meinhardt in 1972. The "activator" $u_1$ is a substance for which deviations from its equilibrium state will be amplified in the absence of diffusion or coupling to the inhibitor, that is, $a_{11} > 0$. This is usually referred to as *autocatalysis* or *positive feedback*. The inhibitor returns to equilibrium when perturbed, and the requirement that $a_{11} + a_{22} < 0$ implies that it is "stronger" than the activator; that is, the exponential rate at which it returns to equilibrium is faster than the activator grows. In order for $D_1 a_{22} + D_2 a_{11} > 0$, we must have $D_2 > D_1$: the rate of diffusion of the inhibitor must be larger than the rate of diffusion of the activator. Finally, to have stability of the homogeneous steady state, we required $a_{11}a_{22} - a_{12}a_{21} > 0$. Since $a_{11}a_{22} < 0$, this implies also that $a_{12}a_{21} < 0$. For this we assume that the activator stimulates production of the inhibitor ($a_{21} > 0$) and that the inhibitor limits the production of the activator ($a_{12} < 0$). The combination of fast diffusion of the inhibitor together with its effect on limiting production of activator is termed *lateral inhibition*. A large region of activator will stimulate production of inhibitor that diffuses and reduces production of inhibitor. In the appropriate circumstances, this leads to a nonuniform distribution of activator with local peaks that are small enough to be in balance with the inhibitor whose production they stimulate nearby. The Gierer-Meinhardt model and its followers are nonlinear models that satisfy these conditions, with nonlinearities that prevent unbounded growth of the concentrations of activator and inhibitor.

## 7.3 Pattern Selection: Steady Patterns

The Turing argument does not help much to understand *which* spatial patterns will emerge when diffusion together with chemical reactions destabilizes a homogeneous steady state of concentrations. Leopards have spots, zebras have stripes and there is a profusion of intricate patterns on butterfly wings. Figures 7.2 and 7.3 show examples of these patterns. We can hypothesize that the leopard got its spots from a reaction-diffusion mechanism. More specifically, we want to know which patterns are produced by which reaction-diffusion systems. This information is helpful in investigations of the biological mechanisms underlying animal coat patterns and the differentiation of tissues that takes place during development of an organism. From a mathematical perspective, our entry point is to regard the reaction-diffusion system [7.10] as a dynamical system and seek to extend the concepts for analyzing dynamical systems to *spatially extended* sys-

**Figure 7.2** An example of animal coat patterns: the eastern chipmunk, *Tamias striatus*. (Photograph ©Marie Read, used with permission.)

tems in which spatial pattern and time varying dynamics can interact with one another. Since we have not discussed them, we focus on the patterns themselves first.

Equilibrium solutions of the reaction-diffusion system [7.10] satisfy the equations

$$D_i \left( \frac{\partial^2 c_i}{\partial x^2} + \frac{\partial^2 c_i}{\partial y^2} \right) = f_i(c_1, \ldots, c_k) \qquad [7.14]$$

together with the boundary conditions that were imposed for [7.10]. This is still a system of partial differential equations which may have many solutions. We ask how many solutions there are and how they depend upon the $D_i, f_i$, and the boundary conditions. Once the solutions to [7.14] have been determined, we can examine their stability as solutions of the system [7.10] which includes time dependence. Similar questions arise in many physical problems, and there is an extensive body of mathematics that has been created to help us solve systems of partial differential equations like [7.14]. We draw upon this mathematics to help us get started.

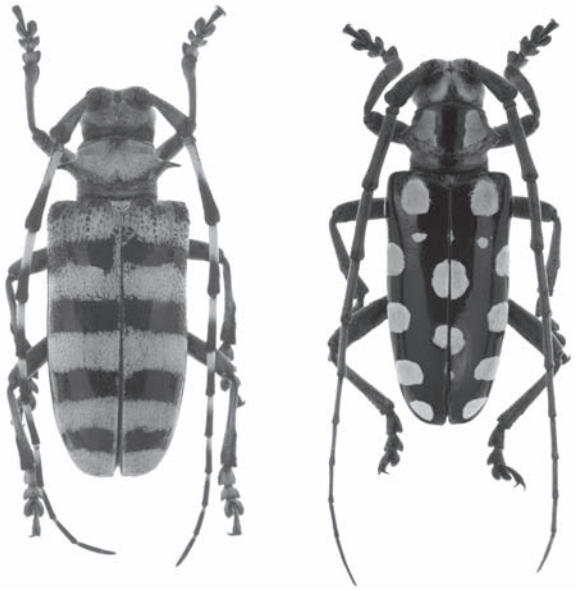

**Figure 7.3** An example of insect color patterns: two beetles from the genus *Anoplophora* with different patterns. Left: *Anoplophora medenbachii* (Ritsema), female, from Java, Indonesia. Right: *Anoplophora mamaua* (Schultze), male, from Mindoro Island, Phillipines. (Photographs by Kent Loeffler, Department of Plant Pathology, Cornell University. From W. Lingafelter and E. R. Hoebeke. 2002. Revision of *Anoplophora* (Coleoptera: Cerambycidae). Entomological Society of Washington, Washington, D.C. Used with permission.)

The simplest version of the *boundary value* problems that we seek to solve is a single, linear equation in one dimension with zero boundary conditions:

$$\begin{aligned} -D\frac{d^2u}{dx^2} + au &= 0 \\ u(0) = U(L) &= 0. \end{aligned} \qquad [7.15]$$

$u(x) \equiv 0$, the function that is identically zero, is always a solution of this equation. We are interested in finding additional solutions that would represent a spatial pattern. If $a > 0$, then the solutions of the equation $Dd^2u/dx^2 + au = 0$ are trigonometric functions of the form $u(x) = c_1 \cos(\sqrt{a/D}x) + c_2 \sin(\sqrt{a/D}x)$. To see whether this $u$ satisfies the boundary conditions of [7.15], we evaluate $u(0) = c_1$ and $u(L) = c_1 \cos(\sqrt{a/D}L) + c_2 \sin(\sqrt{a/D}L)$. Thus the boundary conditions are satisfied if $c_1 = 0$ and $c_2 \sin(\sqrt{a/D}L) = 0$. If $\sqrt{a/D}L$ is an integer multiple of $\pi$, $\sin(\sqrt{a/D}L) = 0$ and the boundary condition at $L$ is satisfied for all values of $c_2$. If $aL^2 = (n\pi)^2$, then the nonzero solutions of the equation have $n - 1$ zeros in the interior of the interval $[0, L]$.

**Exercise 7.2.** Show that if $a < 0$, then the solutions of the equation $Dd^2u/dx^2 + au = 0$ are sums of exponential functions, and the only solutions of the boundary value problem [7.15] is the zero function.

To interpret the implications of this equation, we can regard either $a$ or $L$ as a parameter that varies. For example, if we are interested in a developing organism that is growing and there is diffusion reaction process governed by equation [7.15], then when the organism reaches a critical length $L = n\pi/\sqrt{a/D}$, this process could produce a "segmented" spatial pattern with $n$ segments. However, the model [7.15] seems deficient in two respects: (1) the pattern appears only at the critical lengths $L = n\pi/\sqrt{a/D}$ and then disappears again at longer lengths, and (2) the amplitude of the pattern is not determined.

To "improve" model [7.15], we consider a slight change that makes it nonlinear:

$$\begin{aligned} D\frac{d^2u}{dx^2} + au - u^3 &= 0 \\ u(0) = u(L) &= 0. \end{aligned} \qquad [7.16]$$

The term $u^3$ added to the differential equation is nonlinear. It serves to limit the growth of $u$ due to the reaction terms of the system. Despite the nonlinearity, we can still analyze properties of the system [7.16] by viewing the differential equation as a dynamical system. To do so, we introduce another dependent variable $v$ that represents $du/dx$ and consider the vector field

$$\begin{aligned} \frac{du}{dx} &= v \\ \frac{dv}{dx} &= \frac{-au + u^3}{D}. \end{aligned} \qquad [7.17]$$

Solutions $u(x)$ of the equation $Dd^2u/dx^2 + au - u^3 = 0$ correspond exactly to solutions $(u(x), v(x))$ of [7.17] with $v = du/dx$. The variable $x$ plays the role of the "time" variable in the dynamical system [7.17]. For $a > 0$, the vector field [7.17] has three equilibrium points at $u = -\sqrt{a}, 0, \sqrt{a}$ and $v = 0$. The eigenvalues of the equilibrium at the origin are purely imaginary: $\pm\sqrt{a/D}i$. The key to understanding the phase portrait of system [7.17] is that the function

$$E(u, v) = \frac{1}{2}v^2 + \frac{a}{2D}u^2 - \frac{1}{4D}u^4$$

is constant on trajectories.[1] The level sets of $E$ surrounding the origin are closed curves, so there is a family of trajectories that are periodic orbits. See Figure 7.4. To solve the boundary value problem [7.16], we want to pick out trajectories that

[1] To prove this, use the chain rule to differentiate $E$ with respect to $x$:

$$\frac{dE}{dx} = \frac{\partial E}{\partial u}\frac{du}{dx} + \frac{\partial E}{\partial v}\frac{dv}{dx} = \left(\frac{a}{D}u - \frac{1}{D}u^3\right)v + v\left(\frac{-au + u^3}{D}\right) = 0.$$

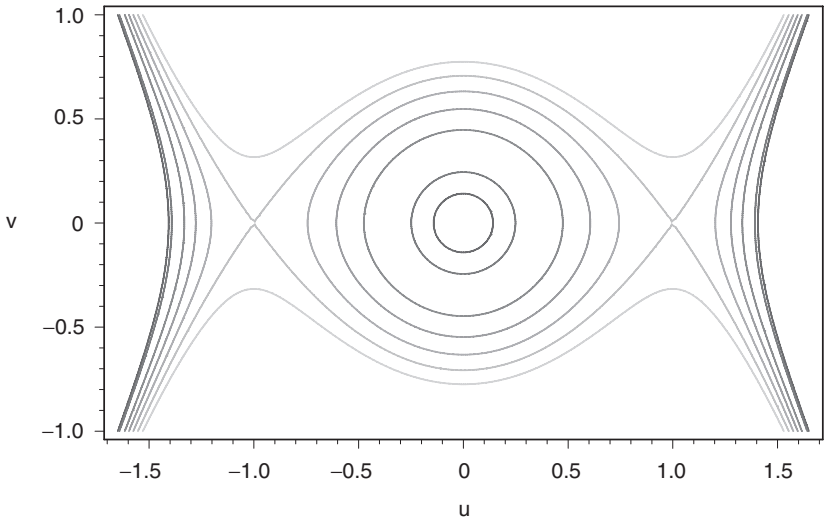


**Figure 7.4** Trajectories of the vector field [7.17] are level curves of the function $E(u, v) = (1/2)v^2 + (a/2D)u^2 - (1/4D)u^4$.

have $u = 0$ at times 0 and $L$. Due to the symmetry of the equation, this will happen if there is an integer $n$ so that the periodic orbit has period $2L/n$. A calculation with *elliptic functions* implies that the periods of the periodic orbits grow as their amplitude grows. The range of values for the periods is from $2\pi/\sqrt{a/D}$, the value determined by the eigenvalues at the origin, to $\infty$, the value obtained as the periodic orbits approach the saddle equilibria. This implies that each time $L = n\pi/\sqrt{a/D}$, a new solution will emerge at the origin and grow in amplitude. Thus, the number of solutions increases as $L$ increases. Our analysis does not address the more difficult question of which of these solutions (if any) is stable as an equilibrium of the reaction-diffusion system [7.10], but it does limit the possible steady patterns.

**Exercise 7.3.** This exercise uses calculus to show that the period $E$ of the solutions to [7.17] increases with amplitude. The periodic solutions lie along the curves $(1/2)v^2 + (a/2D)u^2 - (1/4D)u^4 = c$. A more convenient parametrization is to write

$$2c = \frac{ab^2}{D} - \frac{b^4}{2D}$$

where $b$ is the value of $|u|$ at its intersection with the $u$-axis. Solving for $v$ along this curve,

$$v = \pm\sqrt{\frac{a}{D}(b^2 - u^2) - \frac{1}{2D}(b^4 - u^4)}.$$

Substituting this expression into $du/dx = v$, we obtain

$$\frac{du}{dx} = \pm\sqrt{\frac{a}{D}(b^2 - u^2) - \frac{1}{2D}(b^4 - u^4)}.$$

After a half-period $E/2$ beginning at the point $(u, v) = (-b, 0)$, the solution reaches the point $(u, v) = (b, 0)$. The fundamental theorem of calculus then gives

$$2b = \int_0^{E/2} \frac{du}{dx} dx$$

as an integral formula for determining the value of $E(b)$.

- Apply a change of variables $x = bw$ to "normalize" the domain of $u$ to $[-1, 1]$ in the formula for $E$.
- Differentiate the normalized integral with respect to $b$ to conclude that the period $E$ increases with $b$.

We turn next to the steady spatial patterns produced by solving system [7.14] when diffusion is taking place in a two-dimensional region. The Turing mechanism postulates that the geometry of these solutions determines the spatial patterns observed in developing organisms. This hypothesis can be studied in the context of patterns on the coats of animals like zebras, giraffes and leopards and on the wings of butterflies. The principal biological task in verifying the hypothesis is to identify the diffusible morphogens. This quest has been pursued for decades, but has been given a large boost during the past twenty years by genomic techniques.

When the amplitude of the solutions to equation [7.16] is small, these solutions are almost sinusoidal. This is no accident. Linearization of the equation around the trivial solution leads back to system [7.15]. With two space dimensions the corresponding problem is

$$D\left(\frac{\partial^2 u}{\partial x^2} + \frac{\partial^2 u}{\partial y^2}\right) + au = 0 \qquad [7.18]$$

with boundary conditions $u = 0$ along a curve that bounds a region $R$ in the plane. As in the system [7.15], there will be specific values of $a$ for which there are nonzero solutions. The Turing mechanism postulates that the geometry of these solutions determines the spatial patterns observed in developing organisms. This prompts us to ask how the solutions of this eigenvalue problem depend upon the shape of the region $R$. We resort to numerical methods to solve [7.18] on arbitrary domains, but there do not appear to be any simple answers as to how the solutions depend upon the boundary as was the case for the one-dimensional problem.

The Turing hypothesis is very attractive, but is it correct? Decades of research have given rise to a large body of information without producing a simple yes or no answer. As always, biology is complicated. The organism that has been and continues to be studied the most intensively is the fruit fly *Drosophila*. The development of the segmentation pattern on the abdomen with its bristles and the development of the wing of *Drosophila* have been studied intensively using genetic techniques (Gurdon and Bourillot 2001). One of the key concepts in

Turing's hypothesis is the presence of morphogens whose concentration gradients control the development of specific structures in the organism. Morphogens for *Drosophila* development have been identified conclusively using genetic techniques, along with signaling pathways for their genetic expression and pathways that are "activated" by the morphogens. Identification of these morphogens took a very long time because they are proteins that are active at extremely low concentrations of $10^{-11}$ to $10^{-9}$ M. Spatial patterns of morphogen concentration are difficult to measure, but appear correlated with the structures they induce as predicted by Turing's hypothesis. The morphogens bind to receptors on the surfaces of cells and lead to gene expression through a signaling cascade triggered by the surface binding events. Thus, the cellular response to morphogen concentration is complex with many steps that can interact, each potentially affecting the outcome of the developmental fate of a cell.

The second aspect of the Turing hypothesis is that the mechanism for the transport of morphogens is diffusion. Here the evidence suggests that diffusion is hardly the only transport mechanism. Proteins are large molecules that diffuse slowly, and at the extremely low concentrations of the morphogens, the force of diffusion is small. Moreover, the rates of diffusion are affected by other factors than the morphogen concentration. For example, the Hedgehog protein is a morphogen in *Drosophila* that is modified after translation by cleavage and then covalent linking with cholesterol. These variant forms of Hedgehog have very different diffusion rates in the extracellular matrix of the *Drosophila* embryo (Strigini and Cohen 1999). In addition to diffusion, modes of active transport and "relay" mechanisms that involve repeated secretion and internalization of morphogens from cell to cell seem to be present in some systems. Thus, Turing mechanisms for pattern formation appear more complicated than the simplest reaction-diffusion models in that the morphogens act by triggering whole signaling pathways, and diffusion may be augmented by more "active" transport processes. Nonetheless, one can ask whether observed developmental patterns match solutions of reaction-diffusion equations. In some cases, the answer is yes; for example, in butterfly eyespots (Monteiro et al. 2001). Dynamical models will be a useful tool in unraveling additional details about morphogenesis in developing organisms.

## 7.4 Moving Patterns: Chemical Waves and Heartbeats

Thus far we have considered equilibrium solutions of reaction-diffusion systems. These are by no means the only solutions, or the only ones that are important in biological systems. For example, propagation of action potentials along nerves is a reaction-diffusion process that is essential to the function of the nervous

system. The complex anatomy of biological systems gives rise to diffusion in one-dimensional fibers, two-dimensional sheets, or three-dimensional volumes. Visualizing time-dependent phenomena in three-dimensional tissue is a challenge, so most of the time-dependent spatial patterns that have been studied are two-dimensional patterns on surfaces. The example we discuss here is electrical stimulation of the heartbeat, a vitally important part of our lives. Failure of a coordinated heartbeat leads to death within a matter of minutes. Our hearts are thick enough that this is a three-dimensional process, but we treat the problem as two dimensional as do most studies of spatial patterns of electrical activity in the heart. This section gives a glimpse of the mathematics used to study time-dependent solutions of reaction-diffusion systems, pointing to references that go farther. Throughout the section we work with reaction-diffusion systems in two space dimensions.

The simplest types of time-dependent solution to reaction-diffusion systems are called *traveling waves*. These are solutions in which the time dependence takes the form of a fixed spatial pattern translating in time. If one introduces a coordinate system that translates with the pattern, then the solution of the reaction-diffusion system appears steady in this coordinate system. Analytically, planar traveling waves solve ordinary differential equations that are derived from the reaction-diffusion system in the following way. The orientation of the traveling wave is given by a *wave vector* $(k_x, k_y)$ that specifies the normal direction to the lines on which the solution is constant. We denote the *wave speed* by $s$. The special form of the traveling wave solution is then expressed by stating that the concentrations $c_i(x, y, t)$ are functions of the scalar variable $\xi = k_x x + k_y y - st$. More formally, there are functions $\bar{c}_i$ such that $c_i(x, y, t) = \bar{c}_i(k_x x + k_y y - st) = \bar{c}_i(\xi)$ is a solution of the equation [7.10]. If we substitute $\bar{c}_i$ into [7.10], then we obtain a system of ordinary differential equations with independent variable $\xi$. Using the chain rule, we find

$$\frac{\partial c_i}{\partial t} = \frac{d\xi}{dt}\frac{d\bar{c}_i}{d\xi} = -s\frac{d\bar{c}_i}{d\xi}; \quad \frac{\partial c_i}{\partial x} = k_x\frac{d\bar{c}_i}{d\xi}; \quad \frac{\partial c_i}{\partial y} = k_y\frac{d\bar{c}_i}{d\xi}.$$

Therefore

$$f_i(c_1, \ldots, c_k) + D_i(k_x^2 + k_y^2)\left(\frac{d^2\bar{c}_i}{d\xi^2} + s\frac{d\bar{c}_i}{d\xi}\right) = 0.$$

This is a second-order ordinary differential equation that is converted into a vector field by introducing additional dependent variables for $d\bar{c}_i/d\xi$.

The geometry of traveling waves is determined by their dependence upon the single independent variable $\xi$. In $(x, y, t)$ "space-time," the level surfaces of the $\xi$ are planes whose normal vector is $(k_x, k_y, -s)$. A train of water waves is a good example to help us visualize the behavior of traveling waves. The crests and troughs of the wave are perpendicular to the vector $(k_x, k_y)$ at all times, and they move at a speed $s$ in the direction of this vector. Although traveling waves are

observed in many phenomena, the boundary conditions of physical models are seldom compatible with traveling-wave solutions. Typically, the waves will be deformed near the domain boundary to "match" the constraints imposed by the boundary conditions with the propensity of the medium to support traveling waves.

**Exercise 7.4.** Consider the linear system of reaction diffusion equations

$$\frac{\partial c_1}{dt} = d\left(\frac{\partial^2 c_1}{\partial x^2} + \frac{\partial^2 c_1}{\partial y^2}\right) + ac_1 - bc_2$$

$$\frac{\partial c_2}{dt} = d\left(\frac{\partial^2 c_2}{\partial x^2} + \frac{\partial^2 c_2}{\partial y^2}\right) + bc_1 + ac_2.$$

When does this system have traveling wave solutions of the form

$$c_1(x, t) = \cos(k_x x - st)$$

$$c_2(x, t) = \sin(k_x x - st)?$$

When these solutions exist, find a formula for traveling-wave solutions whose wave vector is parallel to $(k_x, k_y)$.

Planar traveling waves have a space-time symmetry: the wave profiles at different times are translations of each other. We exploit this symmetry to reduce the partial differential equation to an ordinary differential equation when computing the shape of a traveling wave. There are additional mathematical reasons to expect that stable time-dependent solutions of reaction-diffusion systems might have symmetries, and we can search for solutions that have different types of symmetries than traveling waves. Such patterns were first observed in experiments with thin layers of a chemically reacting fluid. Two striking types of solutions with rotational symmetries, *target patterns* and *spiral waves*, are produced by the oscillating *Belousov-Zhabotinsky* (BZ) chemical reaction. Oscillating chemical reactions have been known for about a century (e.g., Bray 1921), but they have been seen as a chemical curiosity at best for much of that period. The laws of thermodynamics tell us that a closed system of reactions eventually comes to equilibrium, just as friction eventually brings a mechanical system that is not acted upon by external forces to rest. Nonetheless, reactions can oscillate for a long time and reactors which receive a steady inflow of reactants can sustain oscillations indefinitely. Epstein and Showalter (1996) survey different types of spatio-temporal phenomena in varied chemical oscillators. The system that has been studied most extensively is the BZ reaction. It was discovered by Belousov in 1951, but his colleagues were skeptical of his work and widespread awareness of his work came only much later [see the account by Winfree (1987)]. The BZ reaction itself involves oxidation of malonic or citric acid by bromate ions, catalyzed by cerium. Addition of an indicator dye to the medium shows the different phases of the reaction as vivid color changes. When the reaction takes place in

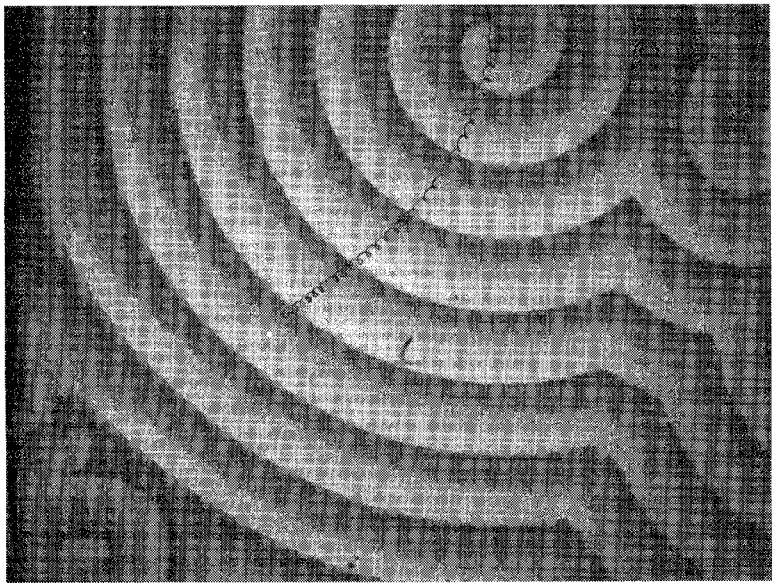

**Figure 7.5** Spiral patterns of the BZ reaction (Reprinted with permission from A. T. Winfree, S. Caudle, G. Chen, P. McGuire, and Z. Szilagyi, Chaos 6: 617 (1996). Copyright 1996, American Institute of Physics).

a thin layer, it is capable of displaying striking spatial patterns like those shown in Figure 7.5. The pattern shown in this figure separates into domains, in each of which a spiral pattern rotates around a "core" at its center, typically with a period on the order of a minute. Target patterns are time-dependent structures in which circular waves propagate radially from a center.

The spatial patterns produced by the BZ system have been studied extensively in the laboratory. There has been a lively interaction between experiment, theory, and simulation surrounding this fascinating system (Field and Burger 1985). Some of the research has sought to construct good dynamical models for the BZ reaction. Producing models that agree quantitatively with the observations has proved to be difficult, despite the fact that the molecules participating in the reaction are small. Another aspect of the research has been to investigate carefully the spatial patterns formed by the BZ reaction and to study their stability. This research draws heavily upon the roles of both topology and symmetry in dynamical systems. Spiral waves have the property that they look steady in a *rotating* coordinate system that rotates with the angular velocity of the waves. However, unlike traveling waves, one cannot reduce the equations describing spiral waves to ordinary differential equations. Thus, research on spiral waves has depended heavily upon numerical simulations of partial differential equations, especially simpler model systems exhibiting spiral waves than those describing

the detailed kinetics of the BZ reaction or the electrical excitability of the heart. Dwight Barkley has written a freely distributed computer code, `ez-spiral`, for the reaction-diffusion system

$$\begin{aligned}\frac{\partial u}{\partial t} &= \frac{\partial^2 u}{\partial x^2} + \frac{\partial^2 u}{\partial y^2} + \epsilon^{-1} u(1-u)\left(u - \frac{v+b}{a}\right) \\ \frac{\partial v}{\partial t} &= D_v\left(\frac{\partial^2 v}{\partial x^2} + \frac{\partial^2 v}{\partial y^2}\right) + u - v\end{aligned} \qquad [7.19]$$

which serves as such a model system.

**Exercise 7.5.** Download the program `ezspiral` and experiment with the patterns that it produces. Alternatively, implement your own program of this type. Implementation requires that the spatial derivatives of the reaction-diffusion system be discretized. The simplest discretizations are given by the finite-difference formulas

$$\frac{\partial u}{\partial t}(x,y,t) \approx \frac{u(x,y,t+h) - u(x,y,t)}{h}$$

$$\frac{\partial v}{\partial t}(x,y,t) \approx \frac{v(x,y,t+h) - v(x,y,t)}{h}$$

$$\begin{aligned}\frac{\partial^2 u}{\partial x^2}(x,y,t) &\approx \frac{(\partial u/\partial x)(x,y,t) - (\partial u/\partial x)(x-k,y)}{h} \\ &\approx \frac{u(x+k,y,t) - u(x,y,t) - (u(x,y,t) - u(x-k,y,t))}{k^2}\end{aligned}$$

$$\begin{aligned}\frac{\partial^2 u}{\partial y^2}(x,y,t) &\approx \frac{(\partial u/\partial y)(x,y,t) - (\partial u/\partial y)(x,y-k,t)}{k} \\ &\approx \frac{u(x,y+k,t) - u(x,y,t) - (u(x,y,t) - u(x,y-k,t))}{k^2}.\end{aligned}$$

Here $h$ is the *time-step* of the method and $k$ is the spacing of points in a regular rectangular mesh used to represent the spatial domain. Simulation of the model requires boundary conditions as well, and these can be difficult to implement for domains with irregular boundaries. `Ezspiral` uses periodic or no-flux boundary conditions in a rectangular domain. The periodic boundary conditions are easiest to implement and correspond to solve the system on a two-dimensional torus that has no boundary. If we ignore arteries and veins, the surface of the heart itself can be regarded as having the topology of a two-dimensional sphere without boundary, but it is harder to discretize the spatial derivatives of the reaction-diffusion equation on a sphere. No flux boundary conditions can be implemented simply and efficiently with a trick. The flux of $u$ flowing between two adjacent sites at $(x, y)$ and $(x-k, y)$ is given by $u(x,y) - u(x-k,y)$. To implement no-flux boundary conditions, we extend the computational domain by adding another row of points to each edge of the boundary. We then assign values to $u$ and $v$ on these extra rows to be equal to those

on the adjacent site inside the domain. This allows us to use the formulas above to compute the spatial derivatives at grid points in the domain along the boundary, and the values that we compute implement the no-flux boundary conditions.

The insights derived from studies of the spatial patterns produced by the BZ reaction have been applied to biological systems, notably by Winfree's theory of ventricular fibrillation in the heart (Winfree 1987). Strong contractions of the ventricles provide the main force for pumping the blood through the lungs and body. Contractions of the heart muscle are triggered by action potentials that propagate by a reaction-diffusion process in a coordinated traveling wave. The action potentials are initiated at the sinoatrial node on the right atrium, spread across the atria to the atrioventricular node, and then spread through the ventricles along the system of Purkinje fibers. Myocardial tissue does not oscillate without stimulation, but fires action potentials in response to a small stimulation. Each spreading wave of electrical excitation is analogous to a grass fire: a fire front propagates through the grass as one burning patch of grass ignites its neighbors. However, the action potentials in the heart are clearly different from grass fires in that the tissue recovers its ability to fire action potentials following a brief refractory period after an action potential. The pumping action of the heart depends on the spatial coherence of the action potential waves.

Heart malfunction can be fatal within minutes or hours. *Ventricular fibrillation* is an immediately life-threatening cardiac arrhythmia in which the spatial pattern of electrical action potentials in the heart becomes more complex and disordered, prompting the heart muscle to quiver. Blood flow largely stops, leading to rapid death. Regulations in the United States now require that many public institutions such as schools and airports have electrical defibrillators available for use. These devices shock the heart in an attempt to synchronize action potentials and restore the normal spatial patterns of action potentials. Many scientists believe that ventricular fibrillation is preceded by the formation of spiral waves of action potentials in the heart. Witkowski et al. (1998) published a striking visualization of spiral waves in the heart. The frequency of the spiral waves is typically much higher than that of the normal heartbeat, a condition called *tachycardia*. Once spiral waves or ventricular fibrillation are established, the heart needs to be given a substantial shock in order to restore normal excitation and contraction. Winfree's 1987 book, *When Time Breaks Down*, is a lively, nontechnical introduction to these theories about ventricular fibrillation.

Propagation of cardiac action potentials can be modeled by systems of equations that couple diffusion of ions to Hodgkin-Huxley-type models for the membrane potential of cardiac cells. These equations have precisely the same form as reaction-diffusion systems, with gating equations for channels and an equation for the membrane potential replacing the chemical reactions in the system. Since the equations have the same form, the same methods can be used in their math-

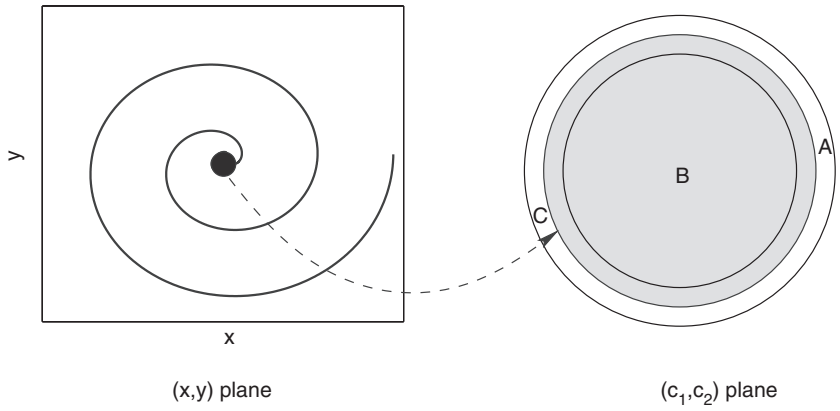


**Figure 7.6** Map of spiral wave in the $(x, y)$ plane into the $(c_1, c_2)$ concentration plane. The dark core of the spiral in the $(x, y)$ plane is mapped into the shaded region in the $(c_1, c_2)$ plane, stretching over the disk $B$. The boundary of the core is mapped onto the curve $C$ bounding the shaded region, making one turn around $B$. All of the points outside the core are mapped into the annulus $A$.

ematical analysis. To the extent that spatial patterns for these systems do not depend upon the details of their "kinetic" terms, we can gain insight into the spatial patterns of cardiac arrhythmias by studying reaction-diffusion systems. Since heart tissue is a difficult medium to work with, we draw inspiration from studies of the BZ reaction to guide investigations of the electrical activity of the heart.

Winfree (1987) describes topological principles related to the spatial patterns formed by time-dependent solutions of reaction-diffusion equations, especially spiral waves. We shall discuss these principles in the setting of systems in which there are two chemical concentrations. At any time, the state of the system gives a map of the "spatial" $(x, y)$ plane into the $(c_1, c_2)$ "concentration" plane. Figure 7.6 illustrates this map. Assume there is a spiral wave pattern in which there is a "core" disk outside of which the concentrations always lie in an annulus $A$ contained in the concentration plane.[2] The complement of an annulus has two components, one bounded and one unbounded. We denote the bounded component of the complement by $B$. Consider the concentration map on the boundary of the core disk. The image will be a curve $C$ in the annulus $A$ that returns to its starting point. The number of times that $C$ winds around $B$ is a *topological* property of $C$ that does not change if $C$ is continuously deformed. Consequently, if the solution evolves continuously as a spiral wave, the image of the concentration map outside the spiral core will continue to surround $B$ the same number of times. Thus, spirals have a propensity to persist: very large per-

[2]An annulus is a region that can be continuously deformed into a region of the form $0 < a < x^2 + y^2 < b$.

turbations are required to destroy them unless they are spontaneously unstable. Typically, instability of the spiral manifests itself in the emergence of more disordered, complex patterns that are described as *spiral turbulence*. Spiral turbulence is widely regarded as a good model for ventricular fibrillation. These properties help explain why defibrillation is required to "restart" a normal sinus rhythm in a heart that is in ventricular fibrillation. They also help explain why a sudden shock like a sharp blow to the chest can sometimes trigger a normal heart to go into a state of fibrillation and cause sudden cardiac death.

Retaining the terminology from the previous paragraph, topology also implies that if $C$ winds around $B$ a nonzero number of times, then the image of the core disk must contain all of $B$. The concentrations in the core of the spiral must be different from those found in the arms of the spiral. This precludes the possibility of developing models for the spiral core in terms of a single angular "phase variable" of concentration. Models with a single phase variable are frequently used to study the synchronization of coupled oscillators (Strogatz 2003), but we cannot model the core of spiral waves in this way. Similar arguments also explain why spirals in the BZ system are typically observed as counter-rotating pairs. The experimental methods that have been used to producing spirals in the BZ system begin with a disturbance in the interior of a homogeneous pattern. Following the disturbance, the net change of phase around the region of disturbance is zero. As spirals develop near the disturbance, the sum of the angular changes produced by their arms must still sum to zero. The simplest pattern that does this is a pair of counter-rotating spirals.

The occurrence of spiral waves was surprising when they were first observed, but even more surprising were observations that show that the spiral cores are capable of coherent motions along flowerlike patterns that resemble those produced by a spirograph! See Figure 7.7. The shape of these meanders has been explained by Barkley as a result of the symmetries of the reaction-diffusion equations (Barkley 1994). In addition to these meandering spirals, in other circumstances the spirals become more unstable and degenerate into disordered patterns that have been described as spatio-temporal turbulence. Using *Fitzhugh-Nagumo* equations equivalent to those used in the `ez spiral` model [7.19], Winfree (1991) produced a diagram of spatio-temporal bifurcations of spirals in a reaction-diffusion system. He hypothesized that disordered patterns evolving from spiral waves are the root cause of ventricular fibrillation in the heart.

As with the Turing mechanism for morphogenesis, we are faced with evaluating the validity of a theory based upon simple dynamical models. The spiral-wave theory of ventricular fibrillation proposes a mechanism for one of the leading causes of death: there are 300,000 people who die of sudden cardiac arrest in the United States yearly. The theory suggests that sudden cardiac death often results from the inability of the heart to pump blood when spiral waves become unstable. Clearly, we want not only a conceptual understanding of ventricular fibrillation

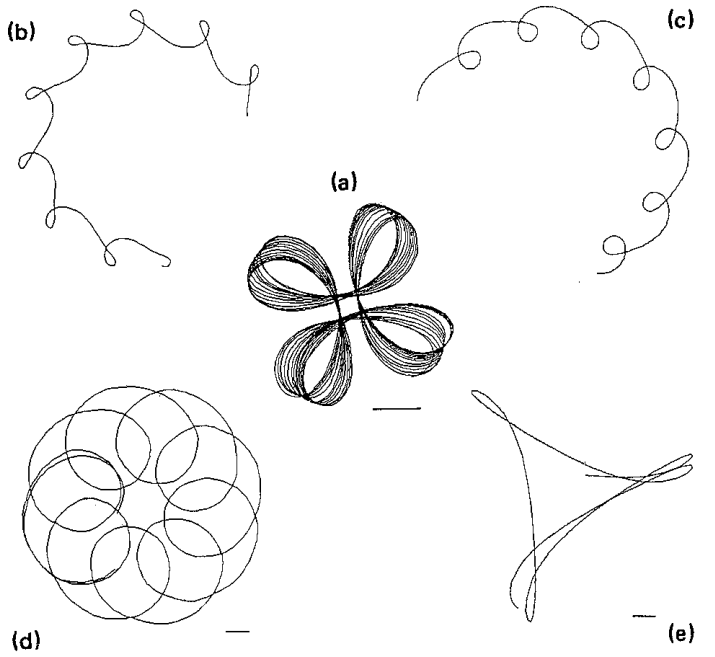


**Figure 7.7** Meandering paths of spiral cores in simulations of a reaction-diffusion system (from Winfree 1991).

but also the means of preventing its occurrence. From a clinical perspective, research on ventricular fibrillation focuses on the breakdown of normal action potential propagation in the sinus rhythm. Two primary causes for block of action potentials are (1) damage to heart tissue that prevents normal conduction of action potentials and (2) changes in cellular properties that lead to abnormally long action potential durations and inadequate time to recover from a refractory period for a normal rhythm. For example, Fox et al. (2002) observed that period-doubling bifurcations in the chemical kinetics seem to lead to instability of wave propagation. Spiral waves and *scroll waves* (Winfree and Strogatz 1983; Keener 1989), their three-dimensional counterparts, lead to ventral tachycardia, degrading the ability of the heart tissue to recover from its refractory period to keep up with the pacing from the wave core. Damaged tissue can give rise to dead regions around which spiral-like waves of action potentials can propagate. Winfree placed emphasis on spiral waves and their topological properties as fundamental aspects of cardiac arrhythmias. Whether or not these topological properties are as important in sudden cardiac death as proposed by Winfree, his theories have had an important influence in focusing attention on action potential propagation as a reaction-diffusion process that is central to cardiac function and disease. Com-

putational models of this process will undoubtedly remain an important tool in research on the heart.

## 7.5 References


Barkley, D. 1994. Euclidean symmetry and the dynamics of rotating spiral waves. Physical Review Letters 72: 164–167.

Barkley, D. ezspiral_3_1.tar.gz, http://www.maths.warwick.ac.uk/ barkley/ez_software.html

Berg, H. C. 1983. *Random Walks in Biology*. Princeton University Press, Princeton, NJ.

Bray, W.C. 1921. A periodic reaction in homogeneous solution and its relation to catalysis. Journal of the American Chemical Society 43: 1262–1267.

Edelstein-Keshet, L. 1988. *Mathematical Models in Biology*. Random House, New York.

Epstein, I. R., and K. Showalter. 1996. Nonlinear chemical dynamics: Oscillations, patterns and chaos, Journal of Physical Chemistry 100: 13132–13147.

Field, R. J., and Burger, M. (eds.). 1985. *Oscillations and Traveling Waves in Chemical Systems*. Wiley, New York.

Fox, J. J., R. F. Gilmour, Jr., and E. Bodenschatz. 2002. Conduction block in one dimensional heart fibers. Physical Review Letters 89: 198101–4.

Gierer, A., and H. Meinhardt. 1972. A theory of biological pattern formation. Kybernetik 12: 30–39.

Goel, N., and N. Richter-Dyn. 1974. *Stochastic Models in Biology*. Springer, New York.

Gurdon, J., and P.-Y. Bourillot. 2001. Morphogen gradient interpretation. Nature 413: 797–803.

Hodges, A. 2000. *Alan Turing: The Enigma* Walker & Co., London.

Keener, J. P. 1989. Knotted scroll wave filaments in excitable media. Physica D 34: 378–390.

Monteiro, A., V. French, G. Smit, P. Brakefield, and J. Metz. 2001. Butterfly eyespot patterns: Evidence for specification by a morphogen diffusion gradient. Acta Biotheoretica 49: 77–88.

Murray, J. D. 1993. *Mathematical Biology*. Springer, New York.

Odell, G., and G. Oster. 1980. The mechanical basis of morphogenesis III: A continuum model of cortical contraction in amphibian eggs. Journal of Mathematical Biology 65–89.

Odell, G., G. Oster, B. Burnside, and P. Alberch. 1980. A mechanical model for epithelial morphogenesis. Journal of Mathematical Biology 9: 291–295.

Odell, G., G. Oster, P. Alberch, and B. Burnside. 1981. The mechanical basis of morphogenesis I: Epithelial folding and invagination. Developmental Biology 85: 446–462.

Strigini, M., and S. Cohen. 1999. Formation of morphogen gradients in the *Drosophila* wing. Seminars in Cell and Developmental Biology. 10: 335–344.

Strogatz, S. 2003. *Sync: The Emerging Science of Spontaneous Order*. Hyperion, New York.

Turchin, P. 1998. *Quantitative Analysis of Movement: Measuring and Modeling Population Redistribution in Animals and Plants*. Sinauer Associates, Sunderland MA.

Turing, A. M. 1952. The chemical basis of morphogenesis. Philosophical Transactions of the Royal Society of London, Series B 237: 37–72.

Winfree, A. T. 1987. *When Time Breaks Down*. Princeton University Press, Princeton, NJ.

Winfree, A. T. 1991. Varieties of spiral wave behavior: An experimentalist's approach to the theory of excitable media. Chaos 1: 303–334.

Winfree, A. T., S. Caudie, G. Chen, P. McGuire, and Z. Szilagy. 1996. Quantitative optical tomography of chemical waves and their organizing centers. Chaos 6: 617–626.

Winfree, A. T., and S. H. Strogatz. 1983. Singular filaments organize chemical waves in three dimensions: 3. Knotted waves. Physica D 9: 333–345.

Witkowski, F. X., L. J. Leon, P. A. Penkoske, W. R. Giles, W. L. Ditto, and A. T. Winfree. 1998. Spatiotemporal evolution of ventricular fibrillation. Nature 392: 78–82.